PHYSICAL REVIEW E **100**, 013105 (2019)

Net fluid flow and non-Newtonian effect in induced-charge electro-osmosis of polyelectrolyte solutions

Huicheng Feng[1,2] and Teck Neng Wong[2,*]

[1]*Unmanned System Research Institute, Northwestern Polytechnical University, Xi'an 710072, China*

[2]*School of Mechanical and Aerospace Engineering, Nanyang Technological University, 50 Nanyang Avenue, Singapore 639798, Singapore*

(Received 4 July 2018; revised manuscript received 9 May 2019; published 12 July 2019)

This paper reports an interesting net fluid flow in the induced-charge electro-osmosis (ICEO) of poly(sodium 4-styrenesulfonate) (NaPSS) solutions measured through microparticle image velocimetry (μPIV). The net fluid flow is attributed to the significantly unequal cations and poly-anions of NaPSS. Owing to the phase delay effect of ions, different flow patterns appear with the alternating electric field. The inflow velocity and outflow velocity are found to be unequal and their relative magnitude shows a dependence on the electric field strength. The ICEO velocity is positively correlated with the NaPSS concentration. As NaPSS introduces the non-Newtonian effect, the well-known quadratic relationship between ICEO velocity and electric field strength in Newtonian fluids breaks. The ICEO velocity varies differently with the electric field strength as the NaPSS concentration changes. These new findings can contribute to the understanding of ICEO of complex fluids, e.g., biofluids.

DOI: 10.1103/PhysRevE.100.013105

I. INTRODUCTION

Induced-charge electro-osmosis (ICEO) has been attracting increasing attention in recent decades owing to its nonlinear relationship with applied electric fields [1–4]. Various ICEO-based applications have been proposed and developed, ranging from micropumps [5], micromixers [6,7], microvalves [8], and micromotors [9] to trappers of microparticles [10] and microdroplets [11]. When a polarizable surface is submerged in an aqueous solution subjected to an external electric field, a fluid flow is generated due to the interaction between the applied electric field and its self-induced electric double layer (EDL) on the surface; this phenomenon is called ICEO. The ζ potential of induced EDL is a function of the applied electric field, which therefore leads to the nonlinearity of ICEO. This nonlinearity promises the existence of ICEO in AC electric fields, which correspondingly enables ICEO to avoid electrochemical reactions commonly encountered in DC electric fields by the conventional linear electro-osmosis. Moreover, it can result in a stronger fluid flow compared to that of the conventional linear electro-osmosis when the applied electric field is large.

Up to now, ICEO is mainly studied regarding Newtonian fluids with the quadratic relationship between ICEO velocity and applied electric field strength (i.e., $u_{\mathrm{ICEO}} \propto E^2$) widely reported [12–16]. While ICEO of non-Newtonian fluids is barely investigated, even though it is more frequently encountered in practical applications, e.g., biomedical [17,18] and chemical analyses [19]. A typical example is a polyelectrolyte solution, which is often used to simulate biopolymers (e.g., DNA and RNA) [20].

To facilitate the application of ICEO in biomicrofluidics, it is of basic significance to study ICEO of polyelectrolyte solutions. Polyelectrolyte solutions are commonly featured with non-Newtonian effect and significantly unequal poly-ions and counter-ions. Electro-osmotic flows of polyelectrolyte solutions have been extensively studied [21,22]. It is reported that the non-Newtonian effect of polyelectrolyte solutions alters the relationship between electro-osmotic velocity and applied electric field [23]. However, Canpolat *et al.* [24] reported that the polymer-containing potassium chloride (KCl) solutions, which are non-Newtonian fluids, follow the same quadratic relationship between ICEO velocity and electric field strength ($u_{\mathrm{ICEO}} \propto E^2$) as the Newtonian fluids.

In addition, Bazant *et al.* [25] predicted that unequal cations and anions of aqueous solutions will lead to a net fluid flow in ICEO of DC electric fields, which is very likely to occur in polyelectrolyte solutions whose poly-ions and counter-ions are significantly unequal. Hashemi Amrei *et al.* [26] found that the unequal mobilities of ions result in an "asymmetric rectified electric field" in oscillating electric fields, which can be a possible reason for the net flow in the ICEO of asymmetric electrolyte solutions. Canpolat *et al.* [24] experimentally studied ICEO of KCl solutions containing polyelectrolytes. Feng *et al.* [16] measured ICEO flow fields of electrolyte solutions with cations and anions of unequal valences (i.e., calcium chloride, $\mathrm{CaCl_2}$) and unequal sizes (i.e., sodium dodecyl sulfate, NaDS). However, both of these studies do not show the net flow. One may raise questions: Is the prediction correct? If so, why do the experiments show a disagreement? Hence, further experimental studies are required for a clarification.

Therefore, to improve the understanding of ICEO of polyelectrolyte solutions, we conducted an experimental study on the ICEO around a gold-coated stainless steel cylinder submerged in poly(sodium 4-styrenesulfonate) (NaPSS) solutions. Both the non-Newtonian effect and significantly unequal poly-ions and counter-ions are analyzed in detail.

---

[*] mtnwong@ntu.edu.sg

2470-0045/2019/100(1)/013105(7)

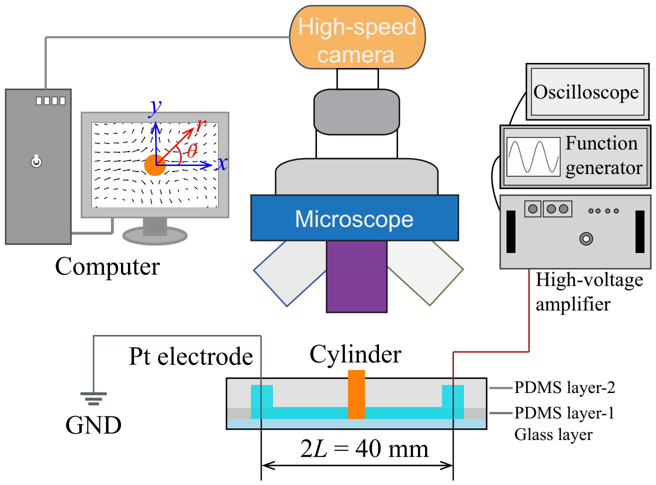

FIG. 1. Experimental setup. The PDMS-glass microchannel was fabricated by soft lithography with the dimensions 0.7 mm (height) × 10 mm (width) × 40 mm (length). A gold-coated stainless steel cylinder of radius $R = 175\,\mu\text{m}$ was positioned in the middle of the microchannel. The ICEO was generated by the AC electric fields applied through the two platinum (Pt) electrodes, captured using a high-speed CCD camera (Vision Research V611) connected to an inverted optical microscope (Leica DM ILM), and processed by the DaVis 8.0 (LaVision) software.

The results clearly capture the net flow, thus verifying the predictions of Bazant *et al.* [25] and Hashemi Amrei *et al.* [26], and they show that the non-Newtonian effect breaks the well-known quadratic relationship between ICEO velocity and electric field strength in Newtonian fluids.

II. EXPERIMENTAL METHODS

We carried out the experiments in a straight rectangular poly(dimethylsiloxane) (PDMS)-glass microchannel and measured ICEO flow fields through a microparticle image velocimetry (μPIV) system. The microchannel was fabricated with a soft lithographic technique. It is composed of one layer of glass slide, two layers of PDMS (Sylgard 184, Dow Corning), and a vertically positioned gold-coated stainless steel cylinder (Fig. 1). Two fluid wells were formed at the microchannel ends. The detailed fabrication process can be found in Feng *et al.* [16].

The poly(sodium 4-styrenesulfonate) (NaPSS, average molecular weight ≈1 000 000, degree of polymerization ≈5000, purity >99%, Sigma-Aldrich) solutions were prepared with deionized (DI) water (18.2 MΩ cm, Milli-Q gradient A10, Millipore), and seeded with spherical fluorescent particles of diameter 3.2 μm (Fluoro-Max, Thermo Fisher Scientific) at a volume fraction of 0.01 vol%. Tween 20 (Sigma-Aldrich) was added into the NaPSS solutions at a volume fraction of 0.005 vol% to avoid particle adhesion on the cylinder surface. The NaPSS solutions were stirred to be well dispersed before injecting into the microchannel for experiments. To eliminate the influence of the possible pressure-driven flow, the experiments were conducted after the fluid within the microchannel became stationary. A function generator (Agilent 33500B) and a high-voltage amplifier (Trek 5/80) were used to created a sinusoidal AC electric field across the microchannel. An oscilloscope (Tektronix TDS210) was used to monitor the applied electric field.

The ICEO flow fields were measured by the widely used μPIV technique. It records the sequential images of the fluid flow seeded with fluorescent particles at a given time interval. The flow field is obtained by processing the recorded images through certain correlation techniques. The present μPIV system is composed of an inverted optical microscope (Leica DM ILM), a high-speed CCD camera (Vision Research V611), a laser source (Litron, wavelength = 527 nm, working frequency range 400 Hz to 10 kHz), and a computer. The particle motions were recorded at rate of 24 Hz by the CCD camera with the image resolution of 1280 × 800 pixels. The 2.5× objective lens ($NA = 0.07$) of the microscope was used to focus on the center plane of the microchannel, providing a field view of $3.64 \times 2.27\,\text{mm}^2$

Some other phenomena, e.g., Brownian motion, dielectrophoresis (DEP), AC electro-osmosis (ACEO), electrothermal (ET) flow, Faradaic polarization, etc., may accompany the ICEO in the microchannel. They may introduce experimental errors into the μPIV measurement of ICEO. The experimental error due to the Brownian motion and DEP motion of tracer particles is small (<0.1%). The ACEO flow on the electrodes and conventional electro-osmosis on the channel wall are negligible under present experimental condition. For detailed analysis, one may refer to Ref. [16]. ET flow is proportional to the fourth order of the applied electric field ($u_{\text{ET}} \propto E^4$) [27]. It would be non-negligible when the conductivity of electrolyte solutions is large. Our previous work shows that the ET flow is negligible in NaCl solutions under the examined experimental conditions [16]. The conductivity of the NaCl solutions is smaller than 0.01 S/m (Fig. 1 of Artemov *et al.* [28]). The conductivity of NaPSS (molecular weight $M_W =$ 1 83 000) solutions within the present examined concentration range is around 0.003 S/m [Fig. 2(d) of Wandrey [29]]. As M_W increases, the conductivity reduces (Fig. 2 of Wandrey [29]). Thus, the conductivity of currently used NaPSS ($M_W =$ 1 000 000) solutions is smaller than 0.003 S/m, which is much smaller than that of the NaCl solutions used by Feng *et al.* [16]. Hence, it is safe to conclude that the ET flow is negligible in this study. Faradaic polarization has been reported to induce a fluid flow exponentially proportional to the applied electric field [30]. It is possible that this fluid flow occurs in the present experiment. However, the experiments of NaCl solutions under similar conditions show purely ICEO flows [16]. It should be reasonable to say that the Faradaic polarization is insignificant in this study. Of course, a systematic theoretical modeling is required to draw a clearer quantitative picture.

III. RESULTS AND DISCUSSION

To facilitate the following discussion, we define a Cartesian coordinate system $(x,\ y)$ whose origin is placed at the cylinder center and the x axis and y axis are rightward and upward, respectively (Fig. 1). Meanwhile, a polar coordinate system $(r,\ \theta)$ is defined with the same origin. The standard ICEO theory predicts that the ICEO velocities of Newtonian fluids

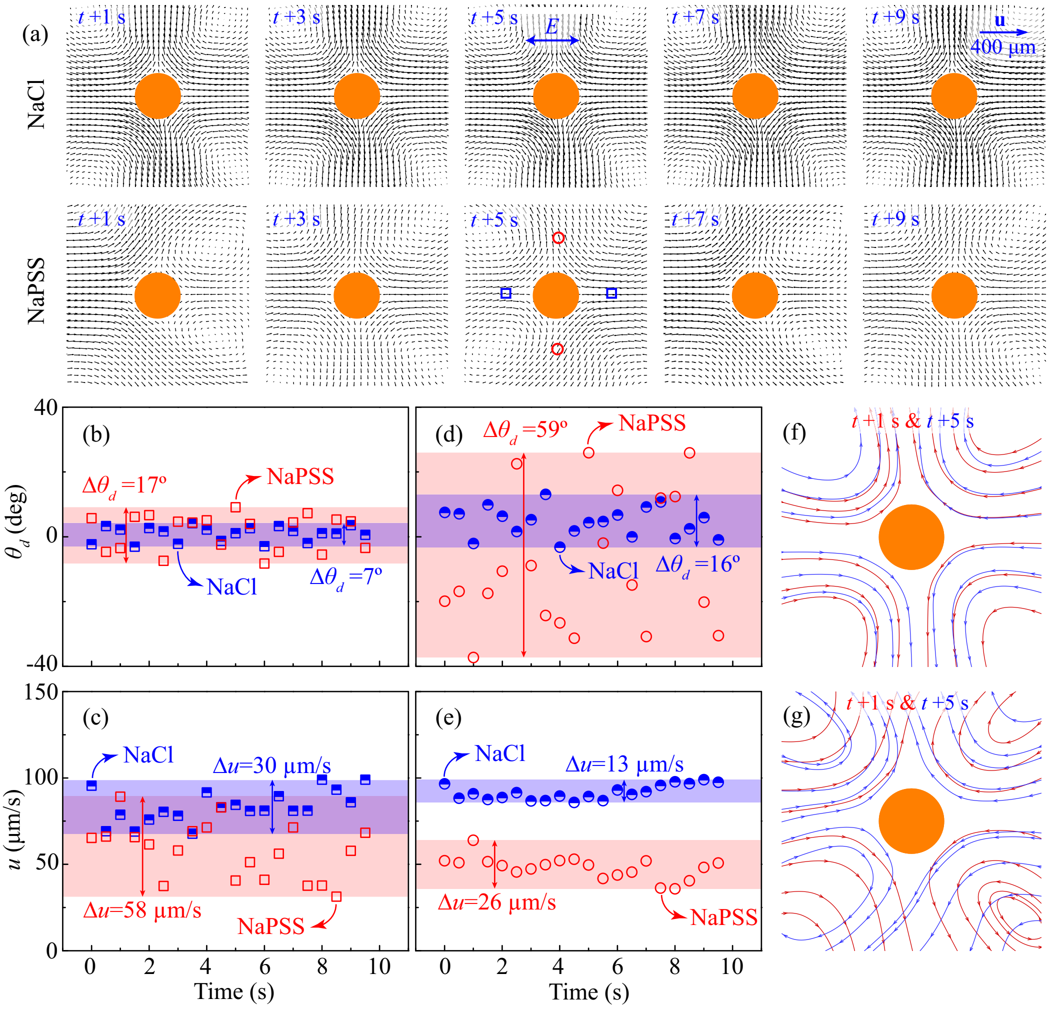

FIG. 2. (a) ICEO flow fields at different times. (b)–(e) Variations of the difference of velocity angle θ_d and velocity magnitude u with time. ICEO flow fields of the (f) NaCl and (g) NaPSS solutions at $t + 1$ and $t + 5$ s (indicated by streamlines). The difference of velocity angle is defined as $\theta_d = \arctan \frac{u_y}{u_x} - \theta_{\rm theor}$, where $\arctan \frac{u_y}{u_x}$ and $\theta_{\rm theor}$ are the experimental and theoretical [Eq. (1)] velocity angles, respectively, which indicate the velocity direction. The squares and circles represent the inflow ($\theta = \pm\pi$) and outflow ($\theta = \pm\pi/2$), respectively. The velocities in (b)–(e) are collected from two fixed points in the inflow ($\theta = \pm\pi$) and outflow ($\theta = \pm\pi/2$) directions. To not lose the generality, the specific positions of the two points are randomly chosen. The concentrations of NaCl and NaPSS solutions are 0.5×10^{-3} mol/L and 2.5×10^{-3} monomol/L, respectively. The electric field strength and frequency are $E = 450\,{\rm V_{p\text{-}p}/cm}$ and $f = 2.0$ kHz, respectively. Please also see Video S1 in the Supplemental Material [33].

around a cylinder are [31,32]

$$u_r = \frac{R(R^2 - r^2)}{r^3} U_0 \cos 2\theta, \quad u_\theta = \frac{R^3}{r^3} U_0 \sin 2\theta, \tag{1}$$

with $U_0 = \frac{\varepsilon_w E^2 R}{\mu(1+f^2\tau_c^2)}$ as the ICEO velocity scale, where ε_w and μ are dielectric constant and viscosity of the electrolyte solutions, respectively, f is the electric field frequency, and τ_c is the cylinder EDL charging time. Equation (1) suggests that the ICEO flow field is symmetric to both the x and y axes, and the inflow velocity ($\theta = \pm\pi$) and outflow velocity ($\theta = \pm\pi/2$) are equal in magnitudes.

From the experimental results, we found that the ICEO flow of NaPSS solutions changes remarkably with time and is solely symmetric to the x axis but asymmetric to the y axis [Fig. 2(a)]. A net fluid flow is generated along the x axis in NaPSS solutions and its direction changes with time [also see Fig. 2(g)]. As time elapses, the net fluid flow can be either toward the positive x axis [e.g., $t + 1$ s of NaPSS solutions in Fig. 2(a)] or the negative x axis [e.g., $t + 5$ s of NaPSS solutions in Fig. 2(a)]. The flow fields of NaCl solutions at different times are also presented in Fig. 2(a) for a comparison. Clearly, the variation with time is insignificant and no net flow appears [also see Fig. 2(f)].

To draw a quantitative picture, we show the variations of both velocity direction and magnitude with time in Figs. 2(b)–2(e). The discrepancy of experimental velocity direction with respect to that of the standard model by Squires and Bazant [31] [i.e., Eq. (1)] is much more significant in the NaPSS solutions than in the NaCl solutions [Figs. 2(b) and 2(d)]. As time elapses, the velocity magnitude varies more significantly than the velocity direction on the x axis [Figs. 2(b) and 2(c)], while it shows otherwise on the y axis [Figs. 2(d) and 2(e)]. The ICEO flow of NaCl solutions roughly follows the direction of

TABLE I. Solute properties of the aqueous solutions.

Solute	Molecular weight (g/mol)	Valence		Ionic radius (nm)	
		cation	anion	cation	anion
Calcium chloride ($CaCl_2$)	111	1	2	0.11 [34]	0.18 [34]
Potassium chloride (KCl)	74.5	1	1	0.15 [34]	0.18 [34]
Sodium dodecyl sulfate (NaDS)	288	1	1	0.11 [34]	1.75 [35]
Poly(ethylene glycol) (PEG)	300				
Poly(diallyldimethylammonium chloride) (PDADMAC)	200 000 ~ 350 000	1587 ~ 2778	1	25 [36]	0.18 [34]
Poly(vinyl sulfonic acid sodium salt) (NaPVSA)	4 000 ~ 6 000	1	28 ~ 42	0.11 [34]	≈100 [37]
Poly(sodium 4-styrenesulfonate) (NaPSS)	1 000 000	1	5 000	0.11 [34]	>100 [38]

Eq. (1) on the x axis [Fig. 2(b)], but shows a larger discrepancy on the y axis [Fig. 2(d)]. While in the NaPSS solutions, the discrepancy of velocity direction is much larger, especially on the y axis. The difference of velocity angle θ_d on the y axis varies from -38° to 26° in the NaPSS solutions [Fig. 2(d)]. This is due to the fact that a net fluid flow appears along the x axis in the NaPSS solutions, which can be evidently seen in Figs. 2(a) and 2(g). As time elapses, the net flow alters its direction between rightward and leftward, which leads to a significant variation of velocity magnitude on the x axis [Fig. 2(c)] and a sign switching of θ_d on the y axis [Fig. 2(d)].

When NaPSS dissolves in DI water, it dissociates into cations Na^+ and poly-anions. The sizes and valences of poly-anions are much larger than those of cations Na^+ as shown in Table I. During the EDL formation, the cations Na^+ and the poly-anions each cover one part of the cylinder surface [Fig. 3(a)]. The poly-anions exist as micelles with many counter-ions attached in NaPSS solutions. Their crowding effect in the EDL leads to a larger local viscosity [39] compared to that of the cation side. It is very likely that the unequal local viscosities will lead to an unequal ICEO slip velocity on the cylinder surface. Moreover, Hashemi Amrei *et al.* [26] reported that the unequal mobilities of ions will results in an "asymmetric rectified electric field" (AREF) in the oscillating electric fields. The AREF generates an electro-osmotic flow in the ICEO flow, i.e., a net flow appears due to the unequal mobilities of ions [Fig. 5(d) of [26]]. González *et al.* [40] reported that unequal mobilities of cations and anions result in a charge density inside the diffusion layer, which co-opts the Faradaic current and affects the slip velocity. However, as aforementioned, the Faradaic current is not strong in the present experiment. Therefore, it is reasonable to conclude that both the unequal local viscosities and the unequal mobilities of ions contribute to the observed net fluid flow along the x axis (i.e., the inflow direction) in the present experiments.

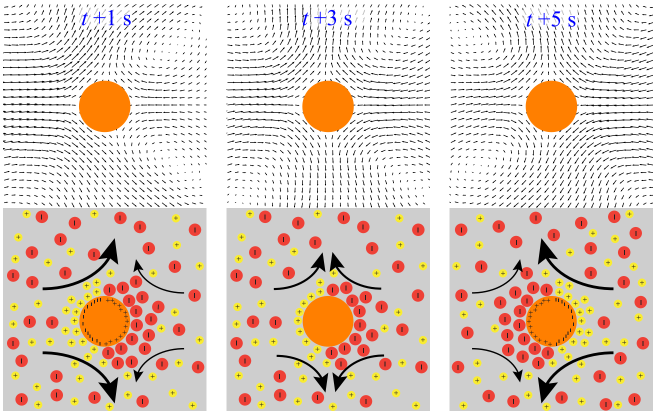

(a) (b) (c)

FIG. 3. Schematic illustration of the different flow patterns in the ICEO of NaPSS solutions.

The AC electric field changes direction with time. Thus, the EDL is decomposed and rebuilt during this process. Ideally speaking, if the ions respond simultaneously to the alternating electric field (i.e., the AC electric field), the net flow will switch directions correspondingly with the same time period of the AC electric field. However, due to the phase delay effect of ions, which has been reported to be significant at low AC frequencies (≈50 Hz) with small ions [41], the time period of the net flow alternating will be larger than that of the AC electric field. What's more, the poly-anions have a smaller mobility due to their larger sizes [39] compared to those of cations Na^+. The different mobilities of Na^+ and poly-anions cause an unequal phase delay effect of ions. Since Na^+ responds faster to the alternating electric field, when the Na^+ side of EDL is partly decomposed, the poly-anion side still mainly remains. Thus, the slip velocity of the Na^+ side is more reduced compared to that of the poly-anion side during the EDL decomposition, which can lead to an equal slip velocity on the cylinder surface. Correspondingly, a symmetric ICEO flow can appear around the cylinder during the EDL rearrangement without any net flow [Fig. 3(b)]. It should be noted that Figs. 2 and 3 show the instantaneous flow fields at different times so as to reveal the net flow in the present ICEO experiments, which can be clearly seen in Video S1 [33]. To achieve a quantitative understanding of this effect, a further theoretical analysis is required.

Canpolat *et al.* [24] and Feng *et al.* [16] measured ICEO flow fields of aqueous solutions with unequal cations and anions in AC electric fields, but did not capture this net flow. The solutions adopted in their experiments are either prepared with solutes of comparable cations and anions (i.e., $CaCl_2$ and NaDS) [16], or containing other comparable cations and anions that suppressed the effect of unequal cations and anions [24]. As shown in Table I, the $CaCl_2$ and NaDS solutions used by Feng *et al.* [16] do not show significant difference in either valences or sizes of cations and anions. The polyelectrolytes, i.e., poly(diallyldimethylammonium chloride) (PDADMAC) and poly(vinyl sulfonic acid sodium salt) (NaPVSA), used by Canpolat *et al.* [24] do have significant differences in both valences and sizes. However, the experiments were conducted

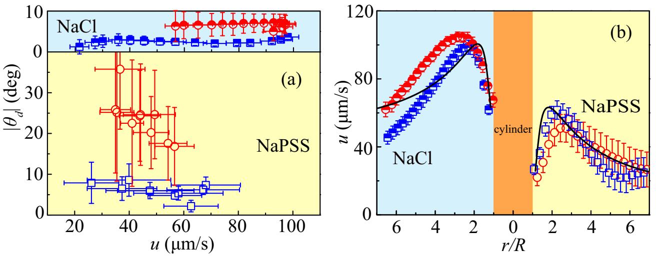

FIG. 4. (a) Variation of the absolute value of velocity angle difference $|\theta_d|$ with the velocity magnitude u. (b) Variation of u along the r direction. The squares and circles represent the inflow ($\theta = \pm\pi$) and outflow ($\theta = \pm\pi/2$), respectively. The curves in (b) are scaled from Eq. (1). The velocities in (a) are randomly picked so as not to lose the generality. The concentrations of NaCl and NaPSS solutions are 0.5×10^{-3} mol/L and 2.5×10^{-3} monomol/L, respectively. The electric field strength and frequency are $E = 450\ \mathrm{V_{p\text{-}p}/cm}$ and $f = 2.0$ kHz, respectively.

in potassium chloride (KCl) solutions containing these polyelectrolytes. The large amount of existing equal-sized ions from KCl (i.e., K^+ and Cl^-) eliminated the effect of unequal cations and anions, thus suppressing the net flow. The present experiment used pure NaPSS solutions, whose cations and anions have significantly unequal valences and sizes (Table I). Thus, the net flow is clearly captured [Figs. 2(a) and 2(g) and 3(a) and 3(c)].

From Figs. 2(c) and 2(e), we can also see that the velocities on the x axis (inflow) and the y axis (outflow) are unequal. This inflow-outflow asymmetry is revealed clearer in Fig. 4. The discrepancy of velocity direction (indicated by $|\theta_d|$) on the y axis is larger than that on the x axis in both the NaCl and NaPSS solutions, while the velocity magnitude u is smaller on the y axis in the NaCl solutions but larger in the NaPSS solutions [also see Fig. 4(b)]. Such inflow-outflow asymmetries of ICEO have been numerically predicted by Davidson *et al.* [42] and experimentally observed by Peng *et al.* [43] and Feng *et al.* [16]. Peng *et al.* [43] reported that the inflow velocity is smaller than the outflow velocity around a sphere submerged in water. Feng *et al.* [16] found that the inflow velocity can be either smaller or larger than the outflow velocity depending on the electrolyte concentration, electrolyte species, and electric field strength and frequency. Through a detailed analysis, we found that as the electric field increases, the inflow velocity is smaller at first and then becomes larger than the outflow velocity in NaPSS solutions [Figs. 5(b) and 5(d)].

The quadratic relationship between ICEO velocity and applied electric field strength ($u_{\mathrm{ICEO}} \propto E^2$) has been well-recognized in Newtonian fluids surrounding conducting surfaces. The situation alters when the fluids are non-Newtonian due to the complex rheology. The NaPSS solutions are power-law fluids. Their generalized Smoluchowski velocity is expressed as [23]

$$u_s = n\kappa^{\frac{1-n}{n}}\left(-\frac{\varepsilon_w \zeta E}{m}\right)^{1/n}, \tag{2}$$

where κ^{-1} is the Debye length, ζ is the zeta potential, and n and m are the flow behavior index and the flow consistency index, respectively.

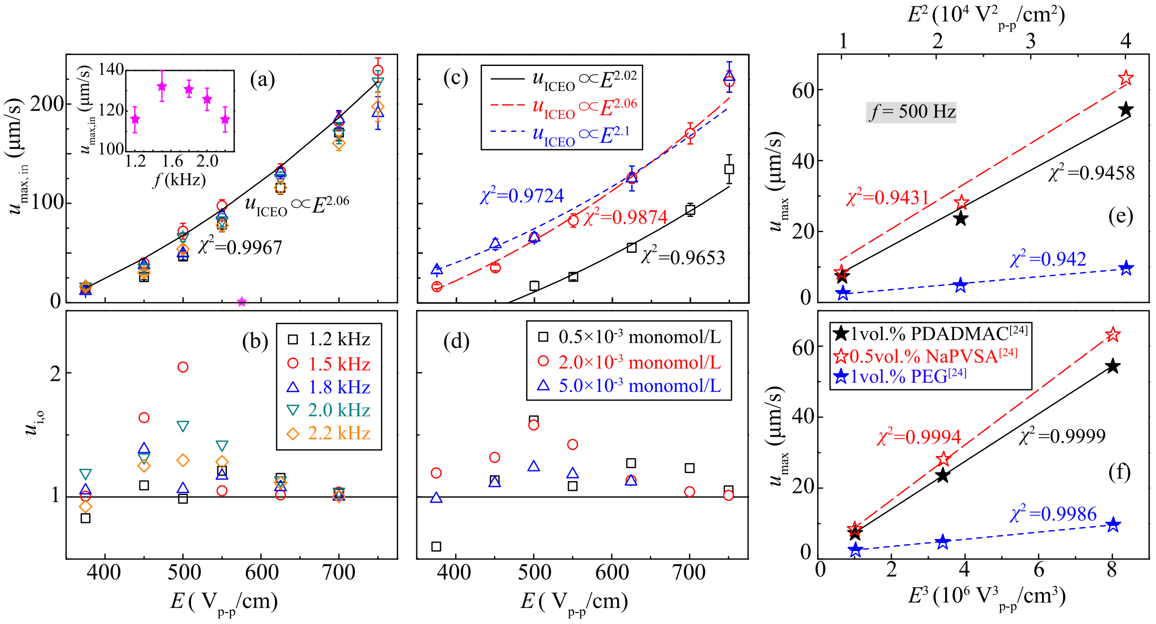

FIG. 5. (a) and (c) Variations of the maximum inflow velocity $u_{\mathrm{max,in}}$ with the electric field strength E at different electric field frequencies f and different NaPSS concentrations c, respectively. (b) and (d) Variations of the inflow-outflow velocity ratio $u_{\mathrm{i,o}}$ with E at different f and c, respectively, where $u_{\mathrm{i,o}} = u_{\mathrm{max,in}}/u_{\mathrm{max,out}}$. (e) and (f) Variations of the maximum velocity u_{max} with the second and third power of electric field strength, respectively, of the $c = 1 \times 10^{-3}$ mol/L KCl solutions containing 1 vol% PDADMAC, 0.5 vol% NaPVSA, and 1 vol% PEG, respectively, at the electric field frequency $f = 500$ Hz [24]. Inset of (a): Variation of $u_{\mathrm{max,in}}$ with f at $E = 625\ \mathrm{V_{p-p}/cm}$. The solid curve in (a) is fitted at $f = 1.5$ kHz. The NaPSS concentration is $c = 2 \times 10^{-3}$ monomol/L in (a) and (b); the electric field frequency is $f = 2.0$ kHz in (c) and (d). The symbol χ^2 indicates the fitting goodness.

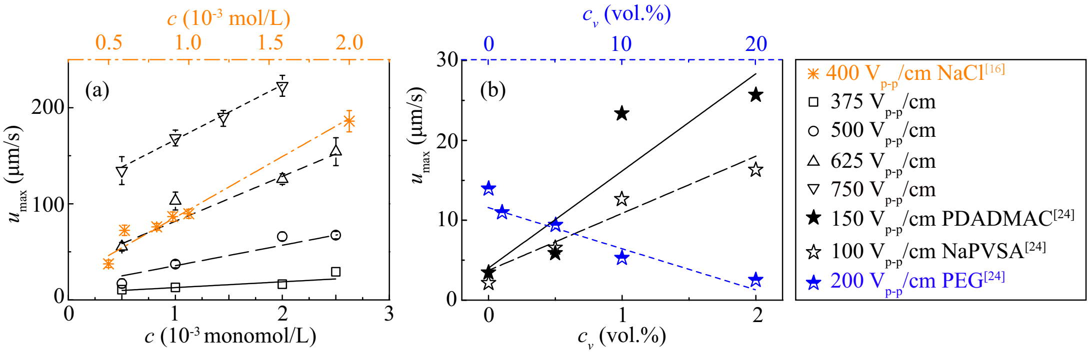

FIG. 6. (a) Variation of the maximum velocity $u_{\max}$ with the NaPSS concentration c at different electric field strengths E, and the NaCl concentration c at $E = 400\ \mathrm{V_{p\text{-}p}/cm}$ [16]. (b) Variation of $u_{\max}$ with the volumetric concentration of different polymers c_v in the $c = 1 \times 10^{-3}$ mol/L KCl solutions [24]. The electric field frequency $f = 2.0$ and 1.5 kHz respectively in (a) and (b).

Since the induced ζ potential of ICEO is proportional to the applied electric field as $\zeta_i \propto ER$, the ICEO velocity of the polymer solutions can be described as

$$u_{\mathrm{ICEO}} \propto n\kappa^{\frac{1-n}{n}}\left(-\frac{\varepsilon_w E^2 R}{m}\right)^{1/n}. \tag{3}$$

It is known that the dielectric constant ε_w of NaPSS solutions changes as the electric field frequency increases due to dielectric relaxations in AC electric fields [44]. However, the variation is negligible at low frequencies ($f < 10$ kHz) [45,46]. Hence, within the narrow range of examined electric field frequency (1.0 ∼ 2.0 kHz), ε_w can be considered as independent of the electric field frequency. As the NaPSS concentration increases, ε_w also increases. Reference [45] showed that ε_w increases from 113.4 to 122.2 as the NaPSS concentration increases from 1.5 to 20.0 monomol/L. Thus, we can conclude that within the examined concentration range (0.5 ∼ 5.0 monomol/L), the variation of ε_w is insignificant.

Therefore, by treating ε_w as a constant, Eq. (3) reveals that $u_{\mathrm{ICEO}} \propto E^{2/n}$. The flow behavior index n is smaller than 1 and decreases as the polymer concentration increases [47]. A smaller n (i.e., a higher NaPSS concentration) shows a greater degree of shear thinning behavior of the NaPSS solutions. We measured the viscosities of NaPSS solutions with a hybrid rheometer (Discovery HR-3, TA Instruments) and obtained m and n through data fitting as listed in Fig. S1 of the Supplemental Material [33]. Clearly, as NaPSS concentration increases, n reduces, which leads to the different relationships between u_{ICEO} and E as shown in Figs. 5(a) and 5(c). Different from our findings, Canpolat *et al.* [24] reported that the ICEO velocity of the polymer-containing KCl solutions (non-Newtonian) is linearly proportional to E^2 [with fitting goodness $\chi^2 \sim 0.94$; Fig. 5(e)]. We revisited their study and redrew the relationship between $u_{\max}$ and E in Fig. 5(e). The better fitting goodness of the linear curves [$\chi^2 > 0.99$ in Fig. 5(f)] suggests that $u_{\max}$ is linearly proportional to E^3 rather than E^2.

The dependence of the present ICEO of non-Newtonian fluids on the electric field frequency is similar to that of Newtonian fluids [16]. As the electric field frequency increases, $u_{\max,\mathrm{in}}$ obtains a peak value although the variation is not significant [inset of Fig. 5(a)]. It is known that ICEO only exists when the frequency of the applied electric field f falls in the range from the charging frequency of the electrodes τ_e^{-1} to the charging frequency of the cylinder τ_c^{-1} [31]. When f is smaller than τ_e^{-1}, the electrodes will be screened by stable EDLs. The electric field cannot be established across the fluid. Thus, ICEO will not be generated. While once f goes beyond τ_c^{-1}, the EDL does not have sufficient time to form on the cylinder surface, therefore, no ICEO occurs either. Hence, it is reasonable that the ICEO achieves a peak value upon increasing the electric field frequency f.

Unlike the well-recognized velocity decay upon increasing the ion concentration in the conventional linear electroosmosis, the dependence of the ICEO velocity on the ion concentration is controversial since both negative [12] and positive [16,24] correlations have been reported. From Fig. 5(c), we can see that the ICEO velocity increases as NaPSS concentration increases. A more detailed analysis on the effect of ion concentration on the ICEO velocity is presented in Fig. 6.

It can be seen that the ICEO velocity increases as the NaPSS concentration increases. Such a positive correlation has been reported on the ICEO of NaCl solutions (Newtonian) by Feng *et al.* [16], which is also presented in Fig. 6(a) as a comparison. Canpolat *et al.* [24] found that the ICEO velocity of the polymer-containing $c = 1 \times 10^{-3}$ mol/L KCl solutions (non-Newtonian) reduces and increases, respectively, upon increasing the concentrations of the non-ionic (i.e., PEG) and ionic (i.e., PDADMAC, NaPVSA) polymers as shown in Fig. 6(b). All three polymers introduce the non-Newtonian effect and increase the fluid viscosity as the polymer concentration increases. The difference is that the ionic polymers also increase the ion concentration upon increasing the polymer concentration. The ICEO velocity of PEG containing KCl solutions reduces as the PEG concentration increases. Hence, it can be concluded that the increase of ICEO velocity in the polymer-containing solutions is due to the increasing ion concentration. Gangwal *et al.* [12] found that, generally, as the NaCl concentration increases, the induced-charge electrophoresis (ICEP) velocity of Janus particles reduces; while when the applied electric field goes beyond 275 $\mathrm{V_{p\text{-}p}/cm}$, the ICEP velocity increases at first and then decreases [Fig. 3(c) of Ref. [16]]. To clarify the underlying physics, detailed theoretical modeling is required. From Fig. 6(a) we can also see that the electric field strength influences the dependence of ICEO velocity on the NaPSS concentration. The slope $\frac{u_{\max}}{c}$

increases as the electric field increases. Clearly, the increasing ion concentration leads to stronger ICEO flows in larger electric fields.

IV. CONCLUSIONS

In this paper, we reported an experimental study on the ICEO of NaPSS solutions in AC electric fields. The experimental results showed that a net fluid flow appears along the inflow direction due to the significantly unequal cations and anions of NaPSS. Moreover, the ICEO flow pattern changes with the alternating electric field due to the phase delay effect of ions. Due to the non-Newtonian effect, the ICEO of NaPSS solutions does not follow the widely reported quadratic relationship between ICEO velocity and applied electric field in Newtonian fluids. The relationship changes as the NaPSS concentration increases. Our analysis also revealed that the ICEO velocity of NaPSS solutions is positively correlated with the NaPSS concentration. The present study can provide a guideline for the application of ICEO in non-Newtonian fluids, e.g., biofluids.

ACKNOWLEDGMENTS

This study is supported by the Singapore Ministry of Education Academic Research Fund Tier 2 research Grant MOE2011-T2-1-036 and the Fundamental Research Funds for the Central Universities.

[1] M. Z. Bazant and T. M. Squires, Curr. Opin. Colloid Interface Sci. **15**, 203 (2010).

[2] C. Zhao and C. Yang, Electrophoresis **32**, 629 (2011).

[3] H. Feng, T. N. Wong, and Marcos, Int. J. Heat Mass Trans. **88**, 674 (2015).

[4] H. Feng and T. N. Wong, Appl. Math. Comput. **333**, 133 (2018).

[5] J. S. Paustian, A. J. Pascall, N. M. Wilson, and T. M. Squires, Lab. Chip **14**, 3300 (2014).

[6] Z. Wu and D. Li, Electrochim. Acta **53**, 5827 (2008).

[7] H. Feng, T. N. Wong, Z. Che, and Marcos, Phys. Fluids **28**, 062003 (2016).

[8] H. Sugioka, Phys. Rev. Applied **3**, 064001 (2015).

[9] H. Feng, T. N. Wong, and Z. Che, Phys. Rev. Fluids **1**, 044103 (2016).

[10] Y. Ren, W. Liu, Y. Jia, Y. Tao, J. Shao, Y. Ding, and H. Jiang, Lab. Chip **15**, 2181 (2015).

[11] D. Das, Z. Yan, N. V. Menon, Y. Kang, V. Chan, and C. Yang, RSC Adv. **5**, 70197 (2015).

[12] S. Gangwal, O. J. Cayre, M. Z. Bazant, and O. D. Velev, Phys. Rev. Lett. **100**, 058302 (2008).

[13] Y. Daghighi, I. Sinn, R. Kopelman, and D. Li, Electrochim. Acta **87**, 270 (2013).

[14] C. Canpolat, S. Qian, and A. Beskok, Microfluid. Nanofluid. **14**, 153 (2013).

[15] C. Canpolat, M. Zhang, W. Rosen, S. Qian, and A. Beskok, J. Fluid. Eng. **135**, 021103 (2013).

[16] H. Feng, Y. Huang, T. N. Wong, and F. Duan, Soft Matter **13**, 4864 (2017).

[17] A. B. Scranton, B. Rangarajan, and J. Klier, in *Biopolymers II*, edited by N.A. Peppas and R.S. Langer (Springer, Berlin, 1995), Vol. 122, pp. 1–54.

[18] D. Yuan, S. H. Tan, R. Sluyter, Q. Zhao, S. Yan, N.-T. Nguyen, J. Guo, J. Zhang, and W. Li, Anal. Chem. **89**, 9574 (2017).

[19] T.-A. Lee, W.-H. Liao, Y.-F. Wu, Y.-L. Chen, and Y.-C. Tung, Anal. Chem. **90**, 2317 (2018).

[20] L. B. Bhuiyan, V. Vlachy, and C. W. Outhwaite, Int. Rev. Phys. Chem. **21**, 1 (2002).

[21] Y. Uematsu, *Electro-Osmosis of Polymer Solutions: Linear and Nonlinear Behavior* (Springer, Berlin, 2017).

[22] F.-M. Chang and H.-K. Tsao, Appl. Phys. Lett. **90**, 194105 (2007).

[23] C. Zhao and C. Yang, J. Non-Newtonian Fluid Mech. **166**, 1076 (2011).

[24] C. Canpolat, S. Qian, and A. Beskok, Microfluid. Nanofluid. **16**, 247 (2014).

[25] M. Z. Bazant, M. S. Kilic, B. D. Storey, and A. Ajdari, Adv. Colloid Interface Sci. **152**, 48 (2009).

[26] S. M. H. Hashemi Amrei, S. C. Bukosky, S. P. Rader, W. D. Ristenpart, and G. H. Miller, Phys. Rev. Lett. **121**, 185504 (2018).

[27] D. Wang, M. Sigurdson, and C. D. Meinhart, Exp. Fluids **38**, 1 (2005).

[28] V. G. Artemov, A. A. Volkov, N. N. Sysoev, and A. A. Volkov, Europhys. Lett. **109**, 26002 (2015).

[29] C. Wandrey, Langmuir **15**, 4069 (1999).

[30] D. Lastochkin, R. Zhou, P. Wang, Y. Ben, and H.-C. Chang, J. Appl. Phys. **96**, 1730 (2004).

[31] T. M. Squires and M. Z. Bazant, J. Fluid Mech. **509**, 217 (2004).

[32] C. Zhao and C. Yang, Phys. Rev. E **83**, 066304 (2011).

[33] See Supplemental Material at http://link.aps.org/supplemental/10.1103/PhysRevE.100.013105 for the movie of ICEO flow fields in 0.5×10^{-3} mol/L NaCl and 2.5×10^{-3} monomol/L NaPSS solutions at $E = 450$ V/cm and $f = 2.0$ kHz, and the viscosities of NaPSS solutions.

[34] R. D. Shannon, Acta Crystallogr. A **32**, 751 (1976).

[35] G. Duplatre, M. F. Marques, and M. Miguel, J. Phys. Chem. **100**, 16608 (1996).

[36] H. Dautzenberg, E. Görnitz, and W. Jaeger, Macromol. Chem. Phys. **199**, 1561 (1998).

[37] I. Moreno-Villoslada, C. Torres, F. González, T. Shibue, and H. Nishide, Macromol. Chem. Phys. **210**, 1167 (2009).

[38] N. Borochov and H. Eisenberg, Macromolecules **27**, 1440 (1994).

[39] Z. Adamczyk, B. Jachimska, T. Jasiński, P. Warszyński, and M. Wasilewska, Colloids Surf. A **343**, 96 (2009).

[40] A. González, A. Ramos, P. García-Sánchez, and A. Castellanos, Phys. Rev. E **81**, 016320 (2010).

[41] H. Sugioka, Phys. Rev. E **94**, 022609 (2016).

[42] S. M. Davidson, M. B. Andersen, and A. Mani, Phys. Rev. Lett. **112**, 128302 (2014).

[43] C. Peng, I. Lazo, S. V. Shiyanovskii, and O. D. Lavrentovich, Phys. Rev. E **90**, 051002(R) (2014).

[44] M. Mandel and T. Odijk, Annu. Rev. Phys. Chem. **35**, 75 (1984).

[45] F. van der Touw and M. Mandel, Biophys. Chem. **2**, 231 (1974).

[46] K. Ito, A. Yagi, N. Ookubo, and R. Hayakawa, Macromolecules **23**, 857 (1990).

[47] Y. Huang, J. Chen, T. N. Wong, and J.-L. Liow, Soft Matter **12**, 6206 (2016).